Local electronic structure and magnetic properties of $LaMn_{0.5}Co_{0.5}O_3$ studied by x-ray absorption and magnetic circular dichroism spectroscopy

T. Burnus,[1] Z. Hu,[1] H. H. Hsieh,[2] V. L. J. Joly,[3] P. A. Joy,[3] M. W. Haverkort,[1] Hua Wu,[1] A. Tanaka,[4] H.-J. Lin,[5] C. T. Chen,[5] and L. H. Tjeng[1]

[1]*II. Physikalisches Institut, Universität zu Köln, Zülpicher Straße 77, 50937 Köln, Germany*

[2]*Chung Cheng Institute of Technology, National Defense University, Taoyuan 335, Taiwan*

[3]*Physical and Materials Chemistry Division, National Chemical Laboratory, Pune 411008, India*

[4]*Department of Quantum Matter, ADSM, Hiroshima University, Higashi-Hiroshima 739-8530, Japan*

[5]*National Synchrotron Radiation Research Center, 101 Hsin-Ann Road, Hsinchu 30076, Taiwan*

(Received 20 September 2007; revised manuscript received 19 December 2007; published 17 March 2008)

We have studied the local electronic structure of $LaMn_{0.5}Co_{0.5}O_3$ using soft-x-ray absorption spectroscopy at the Co-$L_{3,2}$ and Mn-$L_{3,2}$ edges. We found a high-spin Co^{2+}-Mn^{4+} valence state for samples with the optimal Curie temperature. We discovered that samples with lower Curie temperatures contain low-spin nonmagnetic Co^{3+} ions. Using soft-x-ray magnetic circular dichroism, we established that the Co^{2+} and Mn^{4+} ions are ferromagnetically aligned. We also revealed that the Co^{2+} ions have a large orbital moment: $m_{orb}/m_{spin} \approx 0.47$. Together with model calculations, this suggests the presence of a large magnetocrystalline anisotropy in the material and predicts a nontrivial temperature dependence for the magnetic susceptibility.

DOI: 10.1103/PhysRevB.77.125124 PACS number(s): 71.27.+a, 78.70.Dm, 71.70.−d, 75.25.+z

The manganites continue to attract considerable attention from the solid state physics and chemistry community over the last five decades because of their spectacular material properties.[1–4] The parent compound $LaMnO_3$ is an *A*-type antiferromagnetic insulator with orthorhombic perovskite crystal structure. Replacing La by Sr, Ca, or Ba results in multifarious electronic and magnetic properties including the transformation into a ferromagnetic state accompanied by a metal-insulator transition and the occurrence of colossal magnetoresistance.[5,6] Substitution of the magnetic Mn ions by Co also yields ferromagnetism in the $LaMn_{1-x}Co_xO_3$ series. The Curie temperature reaches a maximum for $x=0.5$ ($T_C=220-240$ K).[7–11] This should be contrasted with the end member of this series, namely, the rhombohedral $LaCoO_3$, which is a nonmagnetic insulator at low temperatures, showing yet the well-known spin-state transition at higher temperatures which by itself is the subject of five decades of intensive study.[7,9,12]

Explaining the appearance of ferromagnetism in the manganites by Co substitution is, however, not a trivial issue. Assuming that ordering of the Co and Mn ions had not been achieved for the $x=0.5$ composition, Goodenough *et al.* concluded early on that the ferromagnetism is generated by Mn^{3+}-O-Mn^{3+} superexchange interactions.[7] On the other hand, later magnetic susceptibility and Mn NMR studies suggested that it is the exchange interaction involving the ordering of Co^{2+}-Mn^{4+} transition-metal ions which causes the ferromagnetism in $LaMn_{0.5}Co_{0.5}O_3$.[8,9,13–17]

Only a few high-energy spectroscopic studies are reported for the Co substituted manganites. Using soft-x-ray absorption spectroscopy (XAS), Park *et al.* found in their low Co compositions that the Co ions are divalent, favoring a Mn^{3+}-Mn^{4+} double-exchange mechanism for the ferromagnetism.[18] Extrapolating this Co divalent result to the $x=0.5$ composition would provide support to the suggestion that the ferromagnetism therein is caused by the Co^{2+}-Mn^{4+} exchange interaction. However, no XAS data have been reported so far for this $x=0.5$ composition. Using *K*-edge XAS, Toulemonde *et al.* revealed that the Co ion is also divalent in their hole doped and Co substituted manganite.[19] Yet, these results for the low Co limit have been questioned by van Elp, who claimed that the Co ions should be in the intermediate-spin trivalent state rather than in the high-spin divalent state.[20]

Further discussion is also raised by the work of Joy and co-workers,[21,22] who have synthesized two different single phases of $LaMn_{0.5}Co_{0.5}O_3$ and inferred from a combination of magnetic susceptibility and x-ray photoelectron spectroscopy measurements that the phase with the higher T_C contains high-spin Mn^{3+} and low-spin Co^{3+} ions, while the lower T_C phase has Co^{2+} and Mn^{4+}. Very recently, however, long-range charge ordering has been observed in neutron diffraction experiments by Bull *et al.*[23] and Troyanchuk *et al.*[24] on the high-T_C phase, pointing toward the Co^{2+}-Mn^{4+} scenario. Also, the most recent magnetic susceptibility and *K*-edge XAS data by Kyômen *et al.* favor the presence of essentially Co^{2+}-Mn^{4+} at low temperatures.[25] The issue of Mn/Co ordering including the possible coexistence of ordered and disordered regions remains one of the important topics.[11,26,27] Interesting is that the magnetization of polycrystalline samples of $LaCo_{0.5}Mn_{0.5}O_3$ does not saturate in magnetic fields up to 7 T,[16] and that there are indications for a large magnetic anisotropy.[24]

On the theoretical side, not much work has been carried out so far. A relatively early band-structure study by Yang *et al.* on the $LaMn_{0.5}Co_{0.5}O_3$ system predicted a half-metallic behavior with a magnetic moment of $3.01\mu_B$ for Mn and $0.54\mu_B$ for Co ions, suggesting Mn^{3+}-Co^{3+} valence states.[28] This study, however, was performed before the existence of the charge-ordered crystal structure was reported.[23,24]

Here, we present our experimental study of the local electronic structure of $LaMn_{0.5}Co_{0.5}O_3$ both for the high- and low-T_C phases using the element-specific XAS and x-ray magnetic circular dichroism (XMCD) at the Co-$L_{2,3}$ and Mn-$L_{2,3}$ edges, i.e., transitions from the $2p$ core to the $3d$ valence orbitals. Our objective is not only to establish the

valence and spin states of the Co and Mn ions but also to investigate the possible presence of an orbital moment associated with a Co^{2+} ion, in which case the material should have a large magnetocrystalline anisotropy and a nontrivial temperature dependence of its magnetic susceptibility.

In XAS and XMCD, we make use of the fact that the Coulomb interaction of the $2p$ core hole with the $3d$ electrons is much larger than the $3d$ band width, so that the absorption process is strongly excitonic and therefore well understood in terms of atomiclike transitions to multiplet-split final states.[29–31] Unique to soft-x-ray absorption is that the dipole selection rules are very effective in determining which of the $2p^5 3d^{n+1}$ final states can be reached and with what intensity, starting from a particular $2p^6 3d^n$ initial state ($n=7$ for Co^{2+}, $n=6$ for Co^{3+}, $n=4$ for Mn^{3+}, and $n=3$ for Mn^{4+}). This makes the technique an extremely sensitive local probe, ideal to study the valence[32,33] and spin[12,34–38] character as well as the orbital contribution to the magnetic moment[39–41] of the ground or initial state.

The two single-phase $LaMn_{0.5}Co_{0.5}O_3$ polycrystalline samples were synthesized as described previously[21,22,42] and the single phase nature of the two phases (low-T_C phase and high-T_C phase) were confirmed by temperature dependent magnetization measurements. These measurements showed a single sharp magnetic transition at $T_C=225$ K (called high-T_C phase) for the sample synthesized at 700 °C and a sharp transition at $T_C=150$ K (called low-T_C phase) for the sample synthesized at 1300 °C. On the other hand, more than one magnetic transition or broad magnetic transitions were observed for samples synthesized at other temperatures indicating their mixed phase behavior, as described in Ref. 42. The magnetization at 5 K in a field of 5 T is 50.4 emu/g for the high-T_C phase and 42.4 emu/g for the low-T_C phase. The Co- and Mn-$L_{2,3}$ XAS and XMCD spectra were recorded at the Dragon beamline of the National Synchrotron Radiation Research Center (NSRRC) in Taiwan with an energy resolution of 0.25 eV. The sharp peak at 777.8 eV of the Co-L_3 edge of single crystalline CoO and at 640 eV of the Mn-L_3 of single crystalline MnO were used for energy calibration. The isotropic XAS spectra were measured at room temperature, whereas the XMCD spectra at both the Co-$L_{2,3}$ and the Mn-$L_{2,3}$ edges were measured at 135 K in a 1 T magnetic field with approximately 80% circularly polarized light. The magnetic field makes an angle of 30° with respect to the Poynting vector of the soft x rays. The spectra were recorded using the total electron yield method (by measuring the sample drain current) in a chamber with a base pressure of 2×10^{-10} mbar. Clean sample areas were obtained by cleaving the polycrystals *in situ*.

Figure 1 shows the Co-$L_{2,3}$ XAS spectra of $LaMn_{0.5}Co_{0.5}O_3$ for both the high-T_C [curve (c)] and low-T_C phases [curve (b)]. The spectra were taken at room temperature. For comparison, the spectrum of $LaCoO_3$ in the low-temperature nonmagnetic state [curve (a)] is included as a low-spin trivalent Co reference and also of CoO [curve (d)] as a divalent Co reference. The spectra are dominated by the Co $2p$ core-hole spin-orbit coupling which splits the spectrum roughly in two parts, namely, the L_3 ($h\nu \approx 777-780$ eV) and L_2 ($h\nu \approx 793-796$ eV) white line regions. The line shape of the spectrum depends strongly on

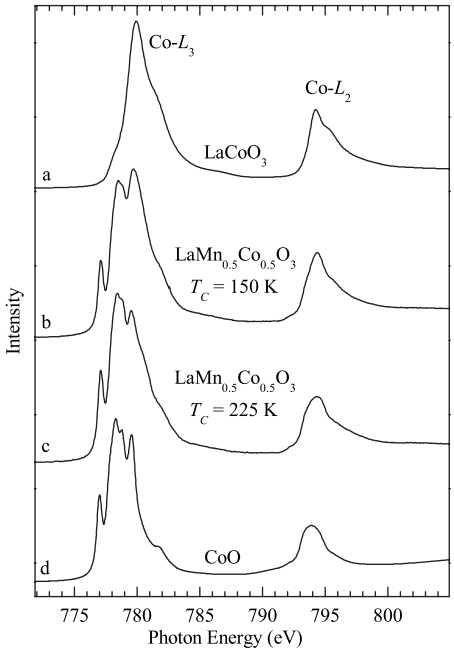

FIG. 1. Co-$L_{2,3}$ XAS spectra of (a) $LaCoO_3$ as a Co^{3+} reference, of the $LaMn_{0.5}Co_{0.5}O_3$ samples with (b) $T_C=150$ K and (c) $T_C=225$ K, and (d) of CoO as a Co^{2+} reference.

the multiplet structure given by the Co $3d$-$3d$ and $2p$-$3d$ Coulomb and exchange interactions, as well as by the local crystal fields and the hybridization with the O $2p$ ligands.

Important is that XAS spectra are highly sensitive to the valence state: an increase of the valence state of the metal ion by one causes a shift of the XAS $L_{2,3}$ spectra by one or more eV toward higher energies.[32,33] This shift is due to a final state effect in the x-ray absorption process. The energy difference between a $3d^n$ ($3d^7$ for Co^{2+}) and a $3d^{n-1}$ ($3d^6$ for Co^{3+}) configuration is $\Delta E=E(2p^6 3d^{n-1}\rightarrow 2p^5 3d^n) - E(2p^6 3d^n \rightarrow 2p^5 3d^{n+1}) \approx U_{pd}-U_{dd} \approx 1-2$ eV, where U_{dd} is the Coulomb repulsion energy between two $3d$ electrons and U_{pd} the one between a $3d$ electron and the $2p$ core hole. In Fig. 1, we see a shift of the "center of gravity" of the L_3 white line to higher photon energies by approximately 1.5 eV in going from CoO to $LaCoO_3$. The energy position and the spectral shape of the high-T_C phase of $LaMn_{0.5}Co_{0.5}O_3$ are very similar to those of CoO, indicating an essentially divalent state of the Co ions.

While the spectral features of the low-T_C phase of $LaMn_{0.5}Co_{0.5}O_3$ are also very similar to those of CoO and the high-T_C phase as far as the low-energy side of the L_3 white line is concerned, this is no longer true for the high energy side. The spectral weight at about 780 eV is increased when one compares the high T_C with the low-T_C phase, and this increase is revealed more clearly by curves (a) of Fig. 2. It is natural to associate this increase with the presence of Co^{3+} species since the $LaCoO_3$ spectrum has its main peak also at 780 eV. In order to verify this in a more quantitative manner, we rescaled the spectrum of the high-T_C phase with respect to that of the low-T_C phase and calculate their difference. We find that a rescaling factor of about 0.8 results in a difference spectrum (dotted blue curve of Fig. 2) which re-

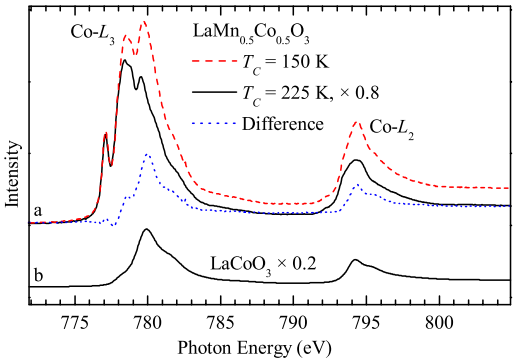

FIG. 2. (Color online) Co-$L_{2,3}$ XAS spectra of (a) the $LaMn_{0.5}Co_{0.5}O_3$ samples with T_C=225 K (solid black curve) and T_C=150 K (dashed red curve), their difference (dotted blue curve), and (b) of $LaCoO_3$ as Co^{3+} reference.

sembles very much the spectrum of $LaCoO_3$. This in turn may be taken as an indication that the low-T_C phase has about 20% of its Co ions in the low-spin trivalent state. This result contradicts the reports in Refs. 21 and 22 which suggested that it was the high-T_C sample which contained trivalent Co ions. The different results coming from the x-ray photoemission (XPS) study[22] could be due to the following reason: Unlike XAS in which the multiplet structure of the Co-$L_{2,3}$ spectra is very characteristic for the Co valence, the XPS yields rather broad and featureless Co $2p$ core-level spectra with very little distinction between Co^{2+} and Co^{3+}. To use XPS core-level shifts to determine the valence state of insulating materials is also not so straightforward due to the fact that the chemical potential with respect to the valence or conduction band edges is not well defined. The present finding of the presence of low-spin Co^{3+} species naturally explains why the low-T_C sample has less than the optimal T_C: the nonmagnetic ions suppress strongly the spin-spin coupling between neighboring metal ions.

Figure 3 shows the room temperature Mn-$L_{2,3}$ XAS spectra of the low-T_C $LaMn_{0.5}Co_{0.5}O_3$ [curve (a)] and the high-T_C $LaMn_{0.5}Co_{0.5}O_3$ [curve (b)] together with $SrMnO_3$ as a tetravalent Mn reference [curve (c)], $LaMnO_3$ as a trivalent Mn reference [curve (d)], and MnO as a divalent Mn reference [curve (e)]. Again, we see a gradual shift of the center of gravity of the L_3 white line to higher energies from MnO to $LaMnO_3$ and further to $SrMnO_3$, reflecting the increase of the Mn valence state from 2+ via 3+ to 4+. The Mn-$L_{2,3}$ spectrum of the high-T_C $LaMn_{0.5}Co_{0.5}O_3$ samples is similar to that of $SrMnO_3$ and $LaMn_{0.5}Ni_{0.5}O_3$,[44] in which a Ni^{2+}/Mn^{4+} valence state was found. The Mn-$L_{2,3}$ XAS spectrum thus reveals an essentially Mn^{4+} state in the high-T_C $LaMn_{0.5}Co_{0.5}O_3$, consistent with the observation of the Co^{2+} valence in the Co-$L_{2,3}$ XAS spectra above, i.e., fulfilling the charge balance requirement.

To investigate whether the presence of Co^{3+} species in the low-T_C $LaMn_{0.5}Co_{0.5}O_3$ is also accompanied by the occurrence of Mn^{3+} ions as charge compensation, we have carried out a similar analysis as for the Co spectra. Figure 4 shows the low-T_C spectrum (red dashed curve) and the high-T_C one (black solid curve) rescaled to 80% of low T_C. Their difference spectrum is shown as the dotted blue curve. We find

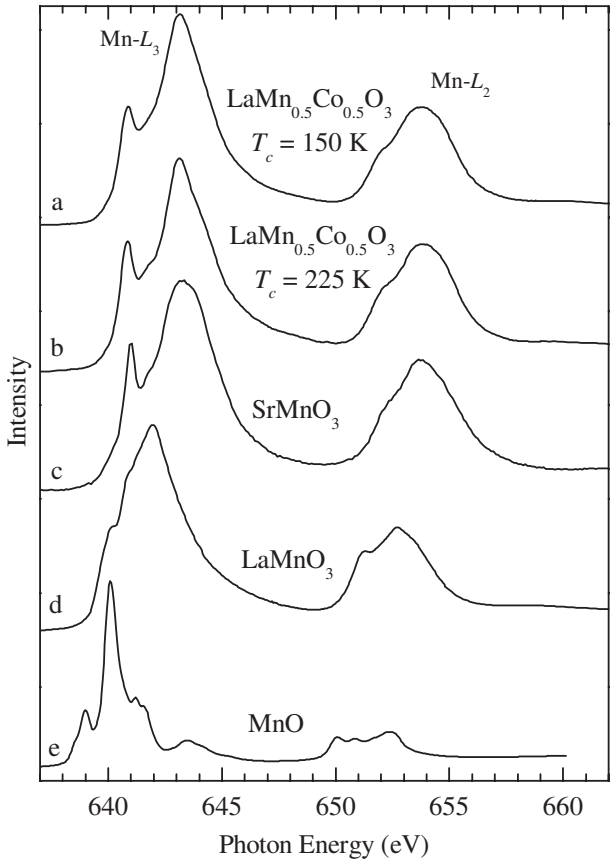

FIG. 3. Mn-$L_{2,3}$ XAS spectra of the $LaMn_{0.5}Co_{0.5}O_3$ sample with (a) T_C=150 K and (b) T_C=225 K together with (c) $SrMnO_3$ (Mn^{4+}, taken from Ref. 43), (d) $LaMnO_3$ (Mn^{3+}), and (e) MnO (Mn^{2+}) for comparison.

that the line shape resembles very much that of the high-T_C sample itself, suggesting that most of the Mn in the low-T_C sample are also tetravalent. This in turn would imply that the low-T_C sample has to have excess of oxygen to account for the presence of the Co^{3+} species. Nevertheless, a closer look reveals that the energy position of the difference spectrum lies between that of the Mn^{4+} and the Mn^{3+} spectra, and that the valley at 641–642 eV, at which energy a typical Mn^{3+} system like $LaMnO_3$ has its maximum, is not so deep. This suggests that in the low-T_C sample, there are also some Mn^{3+} ions or strongly hybridized Mn^{3+} and Mn^{4+} ions. Such a charge compensation for the Co^{3+} could indicate that the ordering of the Mn and Co ions is less than perfect, so that the dislocated Co ions in the Mn^{4+} positions would have smaller metal-oxygen distances, leading to the stabilization of the low-spin trivalent state of the Co.

Having established the valences of the Co and Mn ions, we now focus our attention on their magnetic properties. In the top panel (a) of Fig. 5, we present the XMCD spectra at the Co-$L_{2,3}$ edges of the high-T_C $LaMn_{0.5}Co_{0.5}O_3$ taken at 135 K. The spectra μ^+ (black solid curve) and μ^- (red dashed curve) stand, respectively, for parallel and antiparallel alignments between the photon spin and the magnetic field. One can clearly observe large differences between the two spectra with the different alignments. The difference spectrum, $\Delta\mu=\mu^+-\mu^-$, i.e., the XMCD spectrum, is also shown

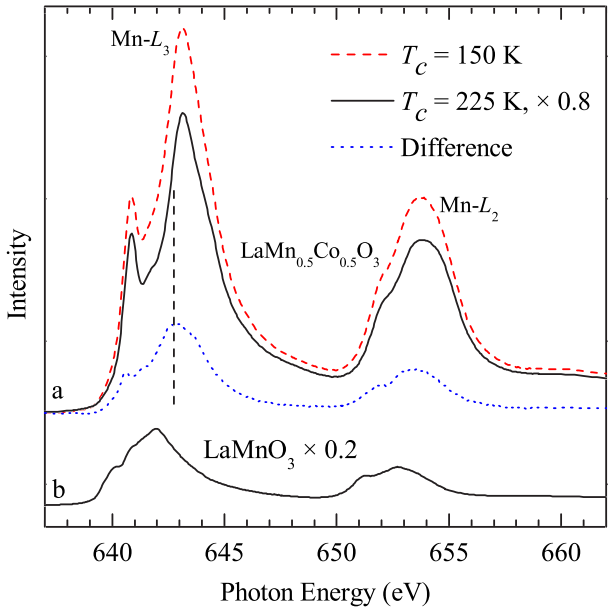

FIG. 4. (Color online) Mn-$L_{2,3}$ XAS spectra of (a) the two $LaMn_{0.5}Co_{0.5}O_3$ samples with T_C=150 K (dashed red curve), T_C =225 K (black solid curve) and their difference (dotted blue curve), and (b) $LaMnO_3$ (Mn^{3+}) for comparison.

(blue dotted curve). In the bottom panel (b) of Fig. 5, we show the XMCD spectra at the Mn-$L_{2,3}$ edges. Also, here we can observe a large XMCD signal. It is important to note that the XMCD is largely negative at both the Co and the Mn L_3 edges, indicating that the Co^{2+} and Mn^{4+} ions are aligned ferromagnetically.

Very interesting about the XMCD at the Co-$L_{2,3}$ edges is that it is almost zero at the L_2 while it is largely negative at the L_3. This is a direct indication that the orbital contribution (L_z,m_{orb}) to the Co magnetic moment must be large. In making this statement, we effectively used the XMCD sum rule derived by Thole *et al.*,[39] in which the ratio between the energy-integrated XMCD signal and the energy-integrated isotropic spectra gives a direct value for L_z. Nevertheless, for a quantitative analysis, it is preferred to extract experimentally the L_z/S_z ratio by making use of an approximate XMCD sum rule developed by Carra *et al.*[45] for the spin contribution ($2S_z$,m_{spin}) to the magnetic moment. This is more reliable than extracting the individual values for L_z and S_z since one no longer needs to make corrections for an incomplete magnetization, due to, for example, possible strong magnetocrystalline anisotropy in a polycrystalline material. The sum rules of Thole *et al.*[39] and Carra *et al.*[45] give for the $m_{\mathrm{orb}}/m_{\mathrm{spin}}$ or $L_z/2S_z$,

$$\frac{m_{\mathrm{orb}}}{m_{\mathrm{spin}}} = \frac{L_z}{2S_z + 7T_z} = \frac{2}{3}\frac{\int_{L_3}\Delta\mu(E)dE + \int_{L_2}\Delta\mu(E)dE}{\int_{L_3}\Delta\mu(E)dE - 2\int_{L_2}\Delta\mu(E)dE}, \tag{1}$$

where T_z denotes the magnetic dipole moment. This T_z for ions in octahedral symmetry is a small number and negligible compared to S_z.[46,47] Using this equation, we extract $m_{\mathrm{orb}}/m_{\mathrm{spin}}$=0.47 out of our Co-$L_{2,3}$ XMCD spectrum. This is a large value and is in fact close to the value of 0.57 for CoO,[49] a compound well known for the important role of the spin-orbit interaction for its magnetic and structural properties.[50–59] The unquenched orbital moment is closely related to the open t_{2g} shell of the $3d^7$ configuration.[60,61]

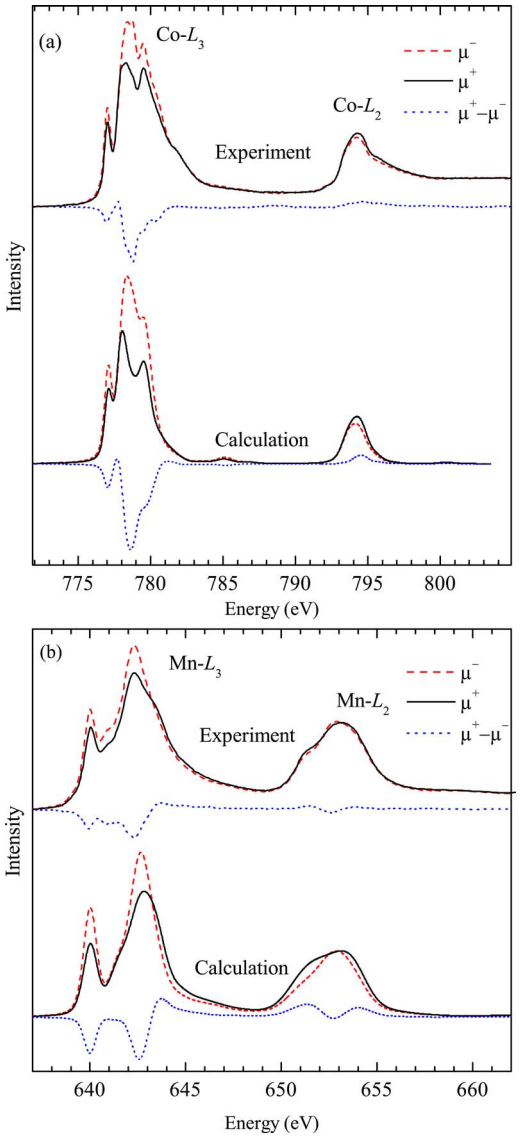

FIG. 5. (Color online) Co-$L_{2,3}$ (a) and Mn-$L_{2,3}$ (b) spectra of $LaMn_{0.5}Co_{0.5}O_3$ taken with circularly polarized x rays at 135 K. The photon spin was aligned parallel (μ^+, black solid) and antiparallel (μ^-, red dashed) to the 1 T magnetic field, respectively; the difference spectra is shown in dotted blue. Top: measured spectra. Bottom: simulated spectra.

Applying the sum rules for the Mn-$L_{2,3}$ XMCD spectra, we obtain $m_{\mathrm{orb}}/m_{\mathrm{spin}}$=0.09. This means that the orbital moment for the Mn^{4+} ions is nearly quenched. Indeed, for the $3d^3$ configuration in the Mn^{4+} compounds, the majority t_{2g} shell is fully occupied and thus a practically quenched orbital moment is to be expected.

To critically check our findings concerning the local electronic structure of the Co and Mn ions, we will explicitly

simulate the experimental XMCD spectra using the configuration interaction cluster model.[29–31] The method uses a CoO_6 and MnO_6 cluster, respectively, which includes the full atomic multiplet theory and the local effects of the solid. It accounts for the intra-atomic $3d$-$3d$ and $2p$-$3d$ Coulomb interactions, the atomic $2p$ and $3d$ spin-orbit couplings, the oxygen $2p$-$3d$ hybridization, and local crystal field parameters. Parameters for the multipole part of the Coulomb interactions were given by the Hartree-Fock values,[29] while the monopole parts (U_{dd}, U_{pd}) as well as the oxygen $2p$-$3d$ charge transfer energies were determined from photoemission experiments on typical Co^{2+} and Mn^{4+} compounds.[62] The one-electron parameters such as the oxygen $2p$-$3d$ and oxygen $2p$-oxygen $2p$ transfer integrals were extracted from band-structure calculations[63] within the local-density approximation (LDA) using the low-temperature crystal structure of the high-T_C phase.[24] The simulations have been carried out using the XTLS 8.3 program[29] with the parameters given in Ref. 64.

Important for the local electronic structure of the Co^{2+} ion is its local t_{2g} crystal field scheme. This together with the spin-orbit interaction determines to a large extent its magnetic properties. To extract the crystal field parameters needed as input for the cluster model, we have performed constrained LDA+U calculations[63] without the spin-orbit interaction. We find that the $zx+xy$ orbital lies lowest, while the yz is located 22 meV and the $zx-xy$ 27 meV higher. Here, we made use of local coordinates in which the z direction is along the long Co-O bond (2.078 Å), the y along the second-longest bond (2.026 Å), and the x along the short bond (1.997 Å). The cluster model finds the easy axis of the magnetization to lie in the yz direction with a single-ion anisotropy energy of about 0.5–1.5 meV, i.e., larger than can be achieved by the applied magnetic field. Since we are dealing with a polycrystalline sample, the sum of spectra taken with the light coming from all directions has to be calculated; we approximated this by summing two calculated spectra: one for light with the Poynting vector along the yz axis and one with the Poynting vector perpendicular to this. The exchange field direction is kept along the yz in both cases.

The results of the cluster model calculations are included in Fig. 5, in the top panel (a) for the Co $L_{2,3}$ edges and the bottom panel (b) for the Mn. One can see that the line shapes of the experimental Co and Mn spectra are well explained by the simulations: all the characteristic features are reproduced. We would like to remark that the experimental XMCD spectra (blue dotted curves) are in general about 30% smaller than the simulated XMCD spectra (blue dotted curves). This is due to the fact that the experimental spectra were *not* corrected for the incomplete degree of circular polarization ($\approx$80%) of the beamline, nor for the fact that magnetic field makes an angle of 30° with respect to the Poynting vector of the light, nor for the reduction of the magnetization at 135 K at which the sample was measured—compared to the calculations which were done at 0 K. From these simulations, we thus can safely conclude that our interpretation for the Co and Mn valences and magnetic moments is sound.

Our finding of a large orbital contribution to the Co magnetic moment has important implications for the interpretation of the magnetic susceptibility data. In most of the studies published so far, one tried to extract magnetic quantum numbers from the magnetic susceptibility data using the Curie or Curie-Weiss law by finding a temperature region in which the inverse of the magnetic susceptibility is linear with temperature. One usually takes the high temperature region. We will show below that this standard procedure will *not* provide the magnetic quantum numbers relevant for the ground state of this material.

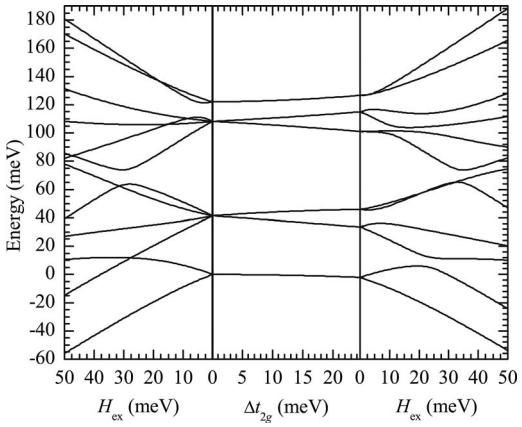

FIG. 6. Energy level diagram of the Co^{2+} ion (left panel) in a cubic field depending on the strength of the exchange field H_{ex}, (middle panel) the effect of lowering the symmetry $[\Delta e_g = 4\Delta t_{2g} = 4(E_{zx-xy,yz} - E_{zx+xy})]$, and (right panel) the low-symmetry energy splitting depending on H_{ex}.

The fact that the $3d$ spin-orbit interaction in this Co material is "active" has as a consequence that the energy difference between the ground state and the first excited state will be of the order of the spin-orbit splitting ζ, which is about 66 meV for the Co^{2+} ion. We have illustrated this in Fig. 6 which shows the energy level diagram of the Co^{2+} ion, both in cubic symmetry (left panel) and in the low-temperature and ferromagnetic state of the $LaMn_{0.5}Co_{0.5}O_3$ system (right panel) where we have used the crystal field scheme as described above.

To demonstrate the consequences of the presence of such a set of low lying excited states, we calculated the magnetic susceptibility χ of the Co^{2+} in cubic symmetry for an applied magnetic field of 0.01 T and without an exchange field. The results are presented in Fig. 7 where we depict also the (apparent) effective magnetic moment μ_{eff} [μ^2_{eff} is defined here as $3k_B$ divided by the temperature derivative of $1/\chi(T)$] and the (apparent) Weiss temperature Θ [Θ is defined here as the intercept of the tangent to the $1/\chi(T)$ curve with the abscissa]. One can clearly observe that $1/\chi(T)$ is not linear with temperature for temperatures between $T_C = 225$ K and roughly 800 K. Only for temperatures higher than 800 K, one can find a Curie-Weiss-like behavior, but then the (apparent) Weiss temperature has nothing to do with magnetic correlations since they were not included in this single ion calculations. Instead, the (apparent) Weiss temperature merely reflects the fact that the first excited states are thermally populated. This means in turn that one cannot directly extract the relevant *ground* state quantum numbers from the high temperature region.

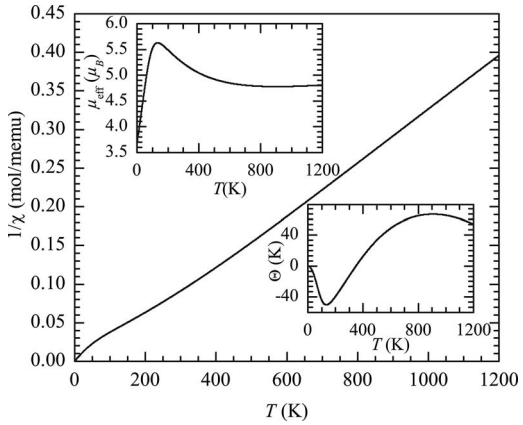

FIG. 7. Calculated inverse susceptibility for a single Co^{2+} ion in a cubic crystal field; (top inset) the (apparent) effective moment μ_{eff} and (bottom inset) the (apparent) Weiss temperature Θ as defined in the text.

In principle, one could hope to find a Curie-Weiss behavior by focusing on the very low temperature region only, e.g., below 50 K, but there one has to take into account that there is a very large van Vleck contribution to the magnetic susceptibility due to the fact that the first excited states are lying very close, i.e., in the range of the spin-orbit splitting. The extrapolation to $T=0$ K would then give the real value for μ_{eff} of the ground state. In the case of $LaMn_{0.5}Co_{0.5}O_3$, however, the presence of ferromagnetism, which already sets in at 225 K, will completely dominate the magnetic susceptibility and thus hinder the determination of μ_{eff} of the ground state using this procedure. Obviously, one can determine in principle the magnetic moments in a ferromagnet from the saturation magnetization, but apparently this is the issue for $LaMn_{0.5}Co_{0.5}O_3$ where one is debating about the importance of Mn/Co disorder and its relationship to reduced magnetizations and less than optimal Curie temperatures.

Another often used "magnetic" technique to determine the moments in this ferromagnetic material is neutron scattering. Troyanchuk *et al.* found a mean value of $2.5\mu_B$ per formula unit ($LaCo_{0.5}Mn_{0.5}O_3$).[24] The authors claimed that this is in good agreement with the Co^{2+}-Mn^{4+} scenario. Indeed, assuming spin-only moments as is generally done (but which is not correct as shown above), one would already expect $3\mu_B$ for a Co^{2+} ion and $3\mu_B$ for a Mn^{4+} ion, totaling to $6\mu_B$, i.e., $3\mu_B$/f.u., which is somewhat larger than the experimental finding and which can be understood consistently if one assumes that the Co-Mn ordering in their sample is not perfect. It is important to note that the low-spin Co^{3+}-Mn^{3+} scenario can be ruled out since this yields only $2\mu_B$/f.u., i.e., too low to explain the experiment. Nevertheless, a Co^{3+}-Mn^{3+} scenario in which the Co^{3+} ion is in the intermediate ($S=1$) or high spin state ($S=2$) cannot be excluded on the basis of the moments measured by the neutrons alone.[38,12]

Our cluster model calculations based on the XAS and XMCD spectra reveal that the Co^{2+} ion has $m_{\text{spin}}=2.12\mu_B$ and $m_{\text{orb}}=0.99\mu_B$ and that the Mn^{4+} has $m_{\text{spin}}=2.84\mu_B$ and $m_{\text{orb}}=0.02\mu_B$, totaling to $2.99\mu_B$/f.u. This is not inconsistent with the magnetization results of Asai *et al.*,[16] if we make an extrapolation to higher magnetic fields as to estimate the saturated total moment. Our result is larger than the neutron results, but also not inconsistent if one is willing to accept that there is an appreciable amount of Co-Mn disorder in the neutron sample. Crucial is that our XAS and XMCD spectra rule out *all* the Co^{3+}-Mn^{3+} scenarios: (1) our Co $L_{2,3}$ spectra give a positive match with those of Co^{2+} compounds, while they do not fit those of low-spin Co^{3+} and high-spin Co^{3+} compounds;[38,12] (2) our Mn $L_{2,3}$ spectra are very similar to those of Mn^{4+} compounds, and very dissimilar to those of Mn^{3+}.

To summarize, we have utilized an element-specific spectroscopic technique, namely, soft-x-ray absorption and magnetic circular dichroism spectroscopy, to unravel the local electronic structure of $LaMn_{0.5}Co_{0.5}O_3$ system. We have firmly established the high-spin Co^{2+}-Mn^{4+} scenario. We have found a very large orbital contribution to the Co magnetic moment, implying a nontrivial temperature dependence for the magnetic susceptibility. We also have revealed that samples with lower Curie temperatures contain low-spin nonmagnetic Co^{3+} ions.

We would like to thank Daniel Khomskii for a critical reading of the paper and Lucie Hamdan for her skillful technical and organizational assistance in preparing the experiments. The research in Cologne is supported by the Deutsche Forschungsgemeinschaft through SFB 608.

[1] G. H. Jonker and J. H. van Santen, Physica (Amsterdam) **16**, 337 (1950).
[2] J. Volger, Physica (Amsterdam) **20**, 49 (1954).
[3] A. P. Ramirez, J. Phys.: Condens. Matter **9**, 8171 (1997).
[4] M. Imada, A. Fujimori, and Y. Tokura, Rev. Mod. Phys. **70**, 1039 (1998).
[5] R. von Helmolt, J. Wecker, B. Holzapfel, L. Schultz, and K. Samwer, Phys. Rev. Lett. **71**, 2331 (1993).
[6] S. Jin, T. H. Tiefel, M. McCormack, R. A. Fastnacht, R. Ramesh, and L. H. Chen, Science **264**, 413 (1994).
[7] J. B. Goodenough, A. Wold, R. J. Arnott, and N. Menyuk, Phys. Rev. **124**, 373 (1961).
[8] G. Blasse, J. Phys. Chem. Solids **26**, 1969 (1965).
[9] G. H. Jonker, J. Appl. Phys. **37**, 1424 (1966).
[10] S. Hébert, C. Martin, A. Maignan, R. Retoux, M. Hervieu, N. Nguyen, and B. Raveau, Phys. Rev. B **65**, 104420 (2002).
[11] R. I. Dass and J. B. Goodenough, Phys. Rev. B **67**, 014401 (2003).
[12] M. W. Haverkort, Z. Hu, J. C. Cezar, T. Burnus, H. Hartmann, M. Reuther, C. Zobel, T. Lorenz, A. Tanaka, N. B. Brookes, H. H. Hsieh, H.-J. Lin, C. T. Chen, and L. H. Tjeng, Phys. Rev. Lett. **97**, 176405 (2006).
[13] N. Nishimori, K. Asai, and M. Mizoguchi, J. Phys. Soc. Jpn. **64**, 1326 (1995).

[14] I. O. Troyanchuk, N. V. Samsonenko, N. V. Kasper, H. Szymczak, and A. Nabialek, J. Phys.: Condens. Matter **9**, 8287 (1997).
[15] I. O. Troyanchuk, N. V. Samsonenko, A. Nabiaiek, and H. Szymczak, J. Magn. Magn. Mater. **168**, 309 (1997).
[16] K. Asai, K. Fujiyoshi, N. Nishimori, Y. Satoh, Y. Kobayashi, and M. Mizoguchi, J. Phys. Soc. Jpn. **67**, 4218 (1998).
[17] I. O. Troyanchuk, L. S. Lobanovsky, D. D. Khalyavin, S. N. Pastushonok, and H. Szymczak, J. Magn. Magn. Mater. **210**, 63 (2000).
[18] J.-H. Park, S.-W. Cheong, and C. T. Chen, Phys. Rev. B **55**, 11072 (1997).
[19] O. Toulemonde, F. Studer, A. Barnab, A. Maignan, C. Martin, and B. Raveau, Eur. Phys. J.: Appl. Phys. **4**, 159 (1998).
[20] J. van Elp, Phys. Rev. B **60**, 7649 (1999).
[21] P. A. Joy, Y. B. Khollam, and S. K. Date, Phys. Rev. B **62**, 8608 (2000).
[22] V. L. Joseph Joly, P. A. Joy, S. K. Date, and C. S. Gopinath, J. Phys.: Condens. Matter **13**, 649 (2001).
[23] C. L. Bull, D. Gleeson, and K. S. Knight, J. Phys.: Condens. Matter **15**, 4927 (2003).
[24] I. O. Troyanchuk, A. P. Sazonov, H. Szymczak, D. M. Többens, and H. Gamari-Seale, J. Exp. Theor. Phys. **99**, 363 (2004).
[25] T. Kyômen, R. Yamazaki, and M. Itoh, Chem. Mater. **15**, 4798 (2003).
[26] T. Kyômen, R. Yamazaki, and M. Itoh, Chem. Mater. **16**, 179 (2004).
[27] C. Autret, K. K. z. J Hejtmánek, M. Marysko, Z. Jirák, M. Dlouhá, and S. Vratislav, J. Phys.: Condens. Matter **17**, 1601 (2005).
[28] Z. Yang, L. Ye, and X. Xie, Phys. Rev. B **59**, 7051 (1999).
[29] A. Tanaka and T. Jo, J. Phys. Soc. Jpn. **63**, 2788 (2004).
[30] F. M. F. de Groot, J. Electron Spectrosc. Relat. Phenom. **67**, 529 (1994).
[31] See the "Theo Thole Memorial Issue", J. Electron Spectrosc. Relat. Phenom. **86**, 1 (1997).
[32] C. T. Chen and F. Sette, Phys. Scr., T **T31**, 119 (1990).
[33] C. Mitra, Z. Hu, P. Raychaudhuri, S. Wirth, S. I. Csiszar, H. H. Hsieh, H.-J. Lin, C. T. Chen, and L. H. Tjeng, Phys. Rev. B **67**, 092404 (2003).
[34] G. van der Laan and B. T. Thole, Phys. Rev. Lett. **60**, 1977 (1988).
[35] B. T. Thole and G. van der Laan, Phys. Rev. A **38**, 1943 (1988).
[36] C. Cartier dit Moulin, P. Rudolf, A. M. Flank, and C. T. Chen, J. Phys. Chem. **96**, 6196 (1992).
[37] H. F. Pen, L. H. Tjeng, E. Pellegrin, F. M. F. de Groot, G. A. Sawatzky, M. A. van Veenendaal, and C. T. Chen, Phys. Rev. B **55**, 15500 (1997).
[38] Z. Hu, H. Wu, M. W. Haverkort, H. H. Hsieh, H. J. Lin, T. Lorenz, J. Baier, A. Reichl, I. Bonn, C. Felser, A. Tanaka, C. T. Chen, and L. H. Tjeng, Phys. Rev. Lett. **92**, 207402 (2004).
[39] B. T. Thole, P. Carra, F. Sette, and G. van der Laan, Phys. Rev. Lett. **68**, 1943 (1992).
[40] C. T. Chen, Y. U. Idzerda, H.-J. Lin, N. V. Smith, G. Meigs, E. Chaban, G. H. Ho, E. Pellegrin, and F. Sette, Phys. Rev. Lett. **75**, 152 (1995).
[41] T. Burnus, Z. Hu, M. W. Haverkort, J. C. Cezar, D. Flahaut, V. Hardy, A. Maignan, N. B. Brookes, A. Tanaka, H.-H. Hsieh, H.-J. Lin, C.-T. Chen, and L. H. Tjeng, Phys. Rev. B **74**, 245111 (2006).
[42] P. A. Joy, Y. B. Khollam, S. N. Patole, and S. K. Date, Mater. Lett. **46**, 261 (2000).
[43] R. K. Sahu, Z. Hu, M. L. Rao, S. S. Manoharan, T. Schmidt, B. Richter, M. Knupfer, M. Golden, J. Fink, and C. M. Schneider, Phys. Rev. B **66**, 144415 (2002).
[44] M. C. Sánchez, J. García, J. Blasco, G. Subías, and J. Perez-Cacho, Phys. Rev. B **65**, 144409 (2002).
[45] P. Carra, B. T. Thole, M. Altarelli, and X. Wang, Phys. Rev. Lett. **70**, 694 (1993).
[46] Y. Teramura, A. Tanaka, and T. Jo, J. Phys. Soc. Jpn. **65**, 1053 (1996).
[47] T_z needs not to be small at the surface [see Crocombette *et al.* (Ref. 48)]. With a probing depth of ≈40 Å, however, the contribution of the surface is a small fraction of that of the bulk, so that ignoring T_z in determining $m_{\mathrm{orb}}/m_{\mathrm{spin}}$ leads to errors not larger than a few percent.
[48] J. P. Crocombette, B. T. Thole, and F. Jollet, J. Phys.: Condens. Matter **8**, 4095 (1996).
[49] G. Ghiringhelli, L. H. Tjeng, A. Tanaka, O. Tjernberg, T. Mizokawa, J. L. de Boer, and N. B. Brookes, Phys. Rev. B **66**, 075101 (2002).
[50] C. G. Shull, W. A. Strauser, and E. O. Wollan, Phys. Rev. **83**, 333 (1951).
[51] Y.-Y. Li, Phys. Rev. **100**, 627 (1955).
[52] W. L. Roth, Phys. Rev. **110**, 1333 (1958).
[53] B. van Laar, Phys. Rev. **138**, A584 (1965).
[54] D. C. Khan and R. A. Erickson, Phys. Rev. B **1**, 2243 (1970).
[55] M. D. Rechtin, S. C. Moss, and B. L. Averbach, Phys. Rev. Lett. **24**, 1485 (1970).
[56] W. Jauch, M. Reehuis, H. J. Bleif, F. Kubanek, and P. Pattison, Phys. Rev. B **64**, 052102 (2001).
[57] J. Kanamori, Prog. Theor. Phys. **17**, 177 (1957).
[58] T. Nagamiya and K. Motizuki, Rev. Mod. Phys. **30**, 89 (1958).
[59] T. Shishidou and T. Jo, J. Phys. Soc. Jpn. **67**, 2637 (1998).
[60] C. J. Ballhausen, *Introduction to Ligand Field Theory* (McGraw-Hill, New York, 1962).
[61] S. I. Csiszar, M. W. Haverkort, Z. Hu, A. Tanaka, H. H. Hsieh, H.-J. Lin, C. T. Chen, T. Hibma, and L. H. Tjeng, Phys. Rev. Lett. **95**, 187205 (2005).
[62] A. E. Bocquet, T. Mizokawa, K. Morikawa, A. Fujimori, S. R. Barman, K. Maiti, D. D. Sarma, Y. Tokura, and M. Onoda, Phys. Rev. B **53**, 1161 (1996).
[63] Hua Wu *et al.* (unpublished).
[64] Parameters CoO_6 cluster: U_{3d3d}=6.5 eV, U_{3d2p}=8.2 eV, Δ=5.5 eV, T_{pp}=0.7 eV, $\Delta_{\mathrm{CF}}^{\mathrm{ionic}}$=450 meV, $\Delta_{t_{2g}}^{\mathrm{ionic}}$=24.5 meV, $\Delta_{zx-xy,yz}^{\mathrm{ionic}}$=5 meV, $\Delta_{e_g}^{\mathrm{ionic}}$=88 meV, $V_{pd\sigma}$=−1.24 eV, $V_{pd\pi}$=0.572 eV, H_{ex}=6.5 meV, and $B_{\mathrm{ext}}^{\mathrm{eff}}$=cos 30° × 1 T. Hartree-Fock results have been used for the Slater integrals, which were reduced to (F_{dd}^2) 90%, (F_{dd}^4) 100%, and (F_p^2, G_{pd}^1, G_{pd}^3) 0.95%. Parameters MnO_6 cluster: U_{3d3d}=5.0 eV, U_{3d2p}=6.0 eV, Δ=−3.0 eV, T_{pp}=0.7 eV, $\Delta_{\mathrm{CF}}^{\mathrm{ionic}}$=0.95 eV, $V_{pd\sigma}$=−1.6 eV, $V_{pd\pi}$=0.74 eV, H_{ex}=6.5 meV, and $B_{\mathrm{ext}}^{\mathrm{eff}}$=cos 30° × 1 T. The Slater integrals were reduced to 70%.